arXiv:hep-ph/0103314v1 29 Mar 2001

Lattice Results on QCD Thermodynamics

Frithjof Karsch*

Fakultät für Physik, Universität Bielefeld, D-33615 Bielefeld, Germany

We review recent results on QCD at finite temperature. Main emphasis is put on a discussion of observables which are of immediate interest to experimental searches for the Quark Gluon Plasma, *i.e.* the phase transition temperature, the equation of state in 2 and 3-flavour QCD, the heavy quark free energy and thermal effects on hadron masses.

1. Introduction

Since many years the thermodynamics of quarks and gluons, the transition between the low temperature hadronic phase and the quark-gluon plasma (QGP) as well as non-perturbative properties of the high temperature phase, have been analyzed through numerical calculations within the framework of lattice regularized QCD. In particular, the studies performed in the pure gauge sector did provide a rather detailed picture of the high temperature plasma phase as a medium of strongly interacting partons which are strongly screened and influenced by non-perturbative effects even at fairly high temperatures.

Over recent years thermodynamic calculations on the lattice have steadily been improved. This partly is due to the much improved computer resources, however equally important has been and still is the development of improved discretization schemes, *i.e.* improved actions. This is of particular relevance for thermodynamic calculations which are not only sensitive to the long distance physics at the phase transition but also probe properties at short distances in calculations of e.g. the energy density or the heavy quark potential. The advantages of improved actions for thermodynamic calculations have been discussed at recent lattice conferences [1,2], this does include improvements of the standard Wilson and staggered fermion actions as well as new developments of chiral actions like the domain wall and overlap fermion formulations. We thus will not go into details of these formulations here. We rather will concentrate on a discussion of results, which may be of direct interest to experimental studies of the quark-gluon plasma. We will discuss the QCD transition temperature and equation of state and will emphasize the quark mass and flavour dependence of these quantities which gives some insight into the mechanisms controlling the transition to the Quark Gluon Plasma. Furthermore we will discuss thermal modifications of the heavy quark free energy and meson masses.

We also refrain from discussing details of the ongoing investigations of the order of the QCD phase transition [3,4], which is first order in the case of three light, degenerate quark flavours and most likely is second order in the case of 2-flavour QCD, although in this latter case questions concerning the universality class of the transition and, in particular,

the role of the axial anomaly for the transition are not yet settled completely. Our current understanding of the QCD phase diagram of 3-flavour QCD at vanishing baryon number density is shown in Figure 1.
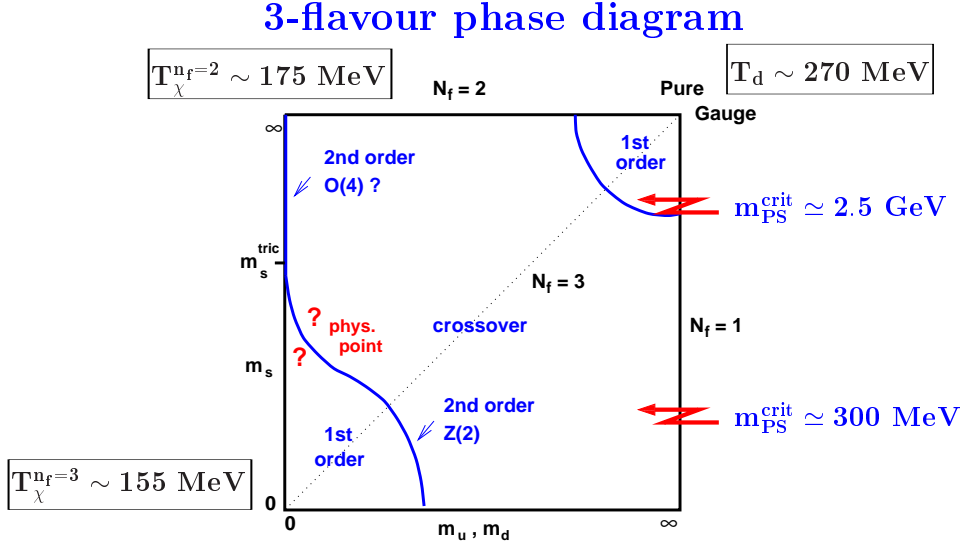
3-flavour phase diagram

Figure 1. The QCD phase diagram of 3-flavour QCD with degenerate (u,d)-quark masses and a strange quark mass m_s.

2. The Critical Temperature and the QCD Phase Diagram

The early calculations of the QCD transition temperature, which have been performed with standard Wilson [5] and staggered [6] fermion actions, led to significant discrepancies of the results. These differences strongly diminished in the newer calculations which are based on improved Wilson fermions (Clover action) [4,6,7], domain wall fermions [8] as well as improved staggered fermions (p4-action) [9]. A compilation of these newer results is shown in Figure 2 for various values of the quark masses. To compare results obtained with different actions the results are presented in terms of a *physical observable*, *i.e.* the ratio of the lightest pseudo-scalar and vector meson masses (m_{PS}/m_V). In Figure 2a we show T_c/m_V obtained for 2-flavour QCD while Figure 2b gives a comparison of results obtained with improved staggered fermions [9] for 2 and 3-flavour QCD. Also shown there is a result for the case of (2+1)-flavour QCD, *i.e.* for two light and one heavier quark flavour degree of freedom. Unfortunately the quark masses in this latter case are still too large to be compared directly with the situation realized in nature. We note however, that the results obtained so far suggest that the transition temperature in (2+1)-flavour QCD is close to that of 2-flavour QCD. The 3-flavour theory, on the other hand, leads to consistently smaller values of the critical temperature, $T_c(n_f = 2) - T_c(n_f = 3) \simeq 20$ MeV. Extrapolation of the transition temperatures to the chiral limit gave

$$\underline{2 - \text{flavour QCD}:} \quad T_c = \begin{cases} (171 \pm 4) \text{ MeV,} & \text{clover-improved Wilson fermions [4]} \\ (173 \pm 8) \text{ MeV,} & \text{improved staggered fermions [9]} \end{cases}$$

$$\underline{3 - \text{flavour QCD}:} \quad T_c = \quad (154 \pm 8) \text{ MeV,} \quad \text{improved staggered fermions [9]}$$
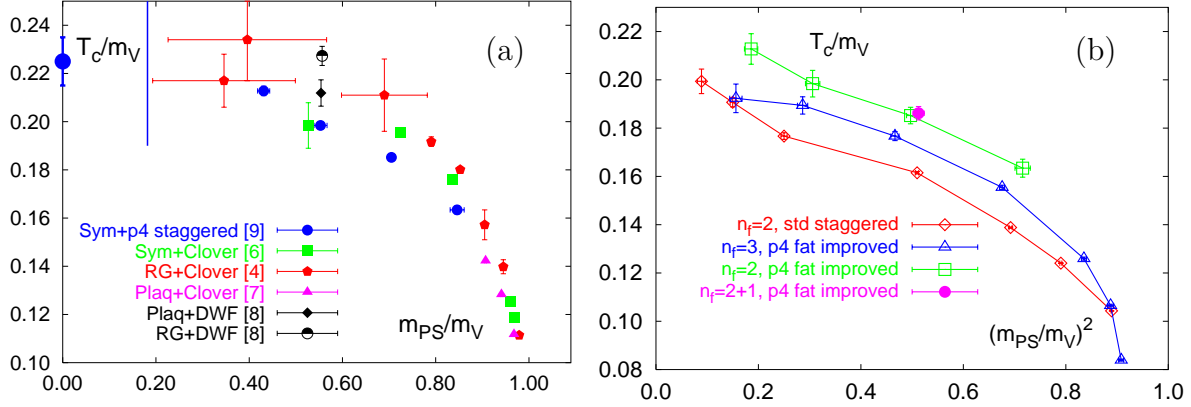
Figure 2. Transition temperatures in units of m_V. In Fig. 2a we give a collection of results obtained for 2-flavour QCD with various fermion actions while Fig. 2b shows a comparison of results obtained in 2 and 3-flavour QCD with unimproved and improved staggered fermion actions. All results are from simulations on lattices with temporal extent $N_\tau = 4$. The large dot drawn for $m_{PS}/m_V = 0$ indicates the result of chiral extrapolations based on calculations with improved Wilson [4] as well as improved staggered [9] fermions. The vertical line shows the location of the physical limit, $m_{PS} \equiv m_\pi$, $m_V \equiv m_\rho$.

Here m_ρ has been used to set the scale for T_c. Although the agreement between results obtained with Wilson and staggered fermions is striking, one should bear in mind that all these results have been obtained on lattice with temporal extent $N_\tau = 4$, *i.e.* at rather large lattice spacing, $a \simeq 0.3$ fm. Moreover, there are uncertainties involved in the ansatz used to extrapolate to the chiral limit. We thus estimate that the systematic error on the value of T_c/m_ρ still is of similar magnitude as the purely statistical error quoted above.

We note from Figure 2 that T_c/m_V drops with increasing ratio m_{PS}/m_V, *i.e.* with increasing quark mass. Apparently this does not reflect the general picture we have for the quark mass (m_q) dependence of T_c. For instance, a simple percolation picture for the QCD transition would suggest that $T_c(m_q)$ or better $T_c(m_{PS})$ will increase with increasing m_q; with increasing m_q also the hadron masses increase and it becomes more difficult to excite the low lying hadronic states. It thus becomes more difficult to create a sufficiently high particle/energy density in the hadronic phase that can trigger a phase (percolation) transition. Such a picture also follows from chiral model calculations [10].

In order to quantify the quark mass dependence of T_c we ideally should find an observable to set the scale for T_c, which itself is not dependent on m_q. This clearly is not the case for m_V, which actually vanishes in the limit $m_q \to \infty$. On the other hand we know from studies of the hadron spectrum and string tension in quenched QCD (SU(3) gauge theory) that these observables agree with experiment and/or QCD phenomenology quite well despite the fact that dynamical light quark contributions are suppressed in this limit. It thus may be expected that (partially) quenched hadron masses or the string tension do provide an almost quark mass independent scale. In fact, this is what tacitly has been assumed when one converts the critical temperature of the SU(3) gauge theory
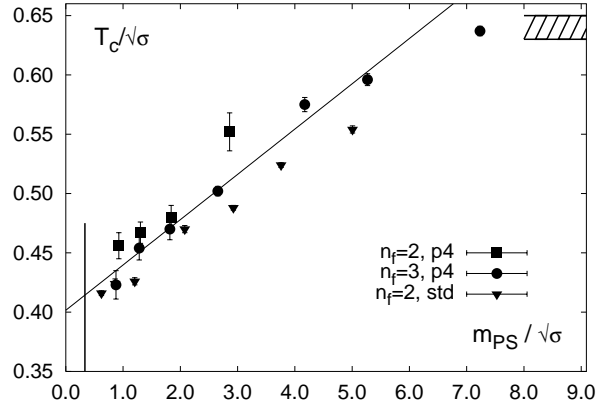
Figure 3. The transition temperature in 2 (filled squares) and 3 (circles) flavour QCD versus $m_{PS}/\sqrt{\sigma}$ using an improved staggered fermion action (p4-action). Also shown are results for 2-flavour QCD obtained with the standard staggered fermion action (open squares). The dashed band indicates the uncertainty on $T_c/\sqrt{\sigma}$ in the quenched limit. The straight line is the fit given in Eq. 2.

$T_c/\sqrt{\sigma} \simeq 0.63$ into physical units[2] as has been done also in Figure 1.

To quantify the quark mass dependence of the transition temperature one may express T_c in units of $\sqrt{\sigma}$. This ratio is shown in Figure 3 as a function of $m_{PS}/\sqrt{\sigma}$. As can be seen the transition temperature starts deviating from the quenched values for $m_{PS} \lesssim (6-7)\sqrt{\sigma} \simeq 2.5$ GeV. We also note that the dependence of T_c on $m_{PS}/\sqrt{\sigma}$ is almost linear in the entire mass interval. Such a behaviour might, in fact, be expected for light quarks in the vicinity of a 2nd order chiral transition where the pseudo-critical temperature depends on the mass of the Goldstone-particle like

$$T_c(m_\pi) - T_c(0) \sim m_\pi^{2/\beta\delta} \; . \tag{1}$$

For 2-flavour QCD the critical indices are expected to belong to the universality class of 3-d, $O(4)$ symmetric spin models and one thus would indeed expect $2/\beta\delta = 1.1$. However, this clearly cannot be the origin of the quasi linear behaviour which is observed for rather large hadron masses and seems to be independent of n_f. Moreover, unlike in chiral models [10] the dependence of T_c on m_{PS} turns out to be rather weak. The line shown in Figure 3 is a fit to the 3-flavour data, which gave

$$(T_c/\sqrt{\sigma})_x = (T_c/\sqrt{\sigma})_0 + 0.04(1) \; x \quad \text{with} \quad x = m_{PS}/\sqrt{\sigma} \quad . \tag{2}$$

For the quark masses currently used in lattice calculations a resonance gas model combined with a suitably chosen percolation criterion would probably be more appropriate to describe the thermodynamics close to T_c.

---

[2]We use here and in the following $\sqrt{\sigma} \simeq 425$ MeV which may be deduced from quenched spectrum calculations ($m_\rho/\sqrt{\sigma} = 1.81$ (4) [12]). Similar values have been obtained from partially quenched calculations in 3-flavour QCD [9].
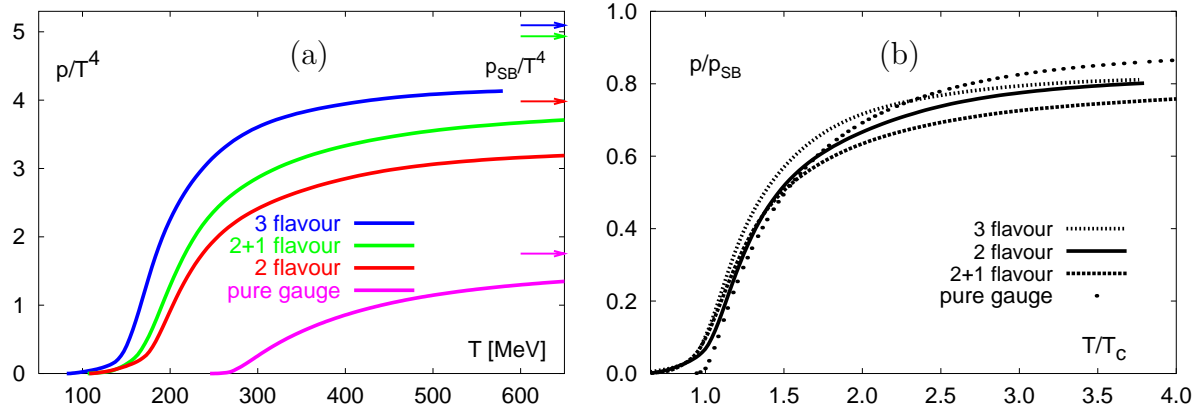
Figure 4. The pressure in QCD with $n_f = 0$, 2 and 3 light quarks as well as two light and a heavier (strange) quark. For $n_f \neq 0$ calculations have been performed on a $N_\tau = 4$ lattice using improved gauge and staggered fermion actions. In the case of the SU(3) pure gauge theory the continuum extrapolated result is shown. Arrows indicate the ideal gas pressure p_{SB} as given in Eq. 3.

3. The Equation of State

When discussing the equation of state of QCD, e.g. the temperature dependence of the energy density (ϵ) and pressure (p), we should at least distinguish three regimes; the high temperature regime ($T \gtrsim 1.5 T_c$), the critical region ($T \simeq T_c$) and the low temperature regime ($T \lesssim 0.9 T_c$). The calculation of ϵ as well as p on the lattice is most difficult below T_c where these observables are exponentially suppressed, which is true even for realistic pseudo-scalar meson masses, $m_{PS} \sim T_c$. We therefore will concentrate on a discussion of the two former temperature regimes.

At high temperature we expect that p/T^4 and ϵ/T^4 will asymptotically approach the free gas limit for a gas of gluons and n_f quark flavours,

$$\frac{\epsilon_{SB}}{T^4} = \frac{3p_{SB}}{T^4} = \left(16 + \frac{21}{2}n_f\right)\frac{\pi^2}{30} \quad . \tag{3}$$

From calculations in the quenched limit, the pure SU(3) gauge theory, we know that the high-T ideal gas limit is reached only very slowly [1]. In fact, for $T \simeq (2-4)T_c$ thermodynamic quantities deviate by about 15% from the limiting ideal gas value. This deviation is too big to be understood in terms of ordinary high temperature perturbation theory which converges badly at these low temperatures [13]. However, it is naturally accounted for in quasi-particle models [14] and resummed perturbative calculations [15]. A similar deviation from ideal gas behaviour has now been found in simulations of QCD with 2 and 3 degenerate quark flavours as well as in a simulation with two light and one heavier quark mass [11]. The results of this calculation which has been performed with an improved gauge and an improved staggered fermion action (p4-action) are shown in Figure 4. As the p4-action is known to lead to much smaller cut-off distortions in the high-T limit than the standard actions, it also becomes meaningful to compare these results with continuum models and perturbative calculations at high temperature [15]. We stress, however, that a final extrapolation to the continuum limit still has to be done
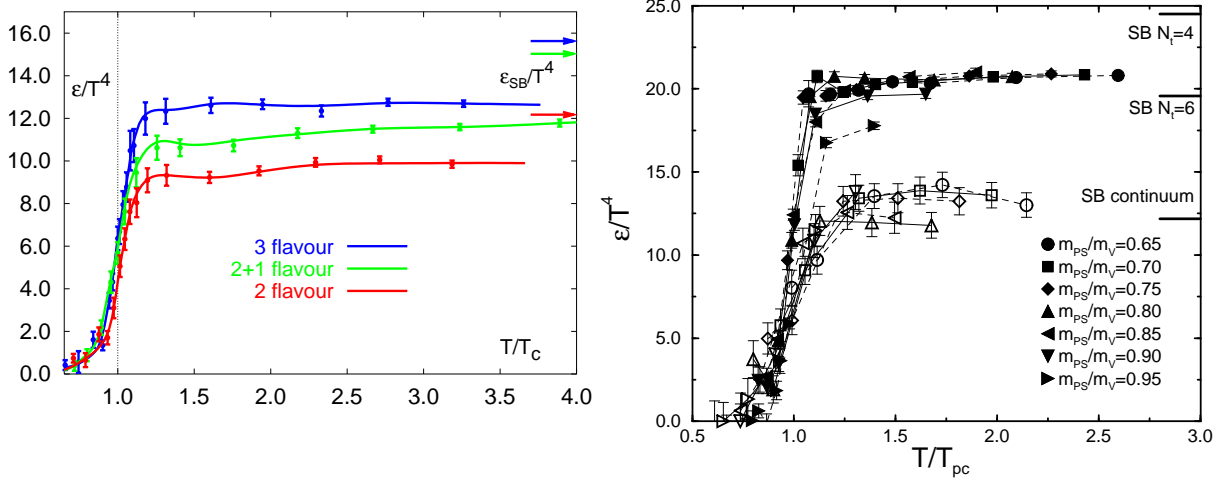
Figure 5. The energy density in QCD. The left (right) figure shows results from a calculation with improved staggered (Wilson) fermions on lattices with temporal extent $N_\tau = 4$ ($N_\tau = 4, 6$). Arrows in the left figure show the ideal gas values ϵ_{SB} as given by Eq. 3.

for QCD with light quarks. From an analysis of the cut-off dependence of the p4-action and the experience gained in the pure gauge sector one expects that the results shown in Figure 4 are still systematically below the final continuum extrapolated result.

The pressure shown in Figure 4a for QCD with different number of flavours as well as for the pure SU(3) gauge theory clearly reflects the strong change in the number of degrees of freedom in the high temperature phase. Moreover, the dependence of T_c on the number of partonic degrees of freedom is clearly visible. In view of this it indeed is striking that p/p_{SB} is almost flavour independent when plotted in units of T/T_c (Figure 4b).

Unfortunately, Wilson actions with similarly good high temperature behaviour have not been constructed so far. The Clover action does not improve the ideal gas behaviour, *i.e.* it has the same infinite temperature limit as the Wilson action. Consequently one observes an overshooting of the ideal gas limit at high temperature which reflects the cut-off effects in the unimproved fermion sector [16]. These cut-off effects are, however, unimportant in the vicinity of the phase transition where correlation lengths become large. It thus makes sense to compare results obtained with different actions in this regime. In Figure 5 we show recent results for the energy density obtained with improved staggered[3] and Wilson [16] fermions. We note that these calculations yield consistent estimates for the energy density at T_c

$$\epsilon_c \simeq (6 \pm 2) T_c^4 \quad . \tag{4}$$

This estimate also is consistent with results obtained for the energy density from calculations with a standard staggered fermion action [17].

---

[3]This figure for staggered fermions is based on data from Ref [11]. Here a contribution to ϵ/T^4 which is proportional to the bare quark mass and vanishes in the chiral limit is not taken into account.

4. Heavy quark free energy and screening below T_c

For the discussion of medium effects on heavy quark bound states in the QGP it is of great importance to calculate thermal modifications of the heavy quark colour singlet potential. Unfortunately this is not directly accessible to lattice calculations, in particular not as a gauge invariant observable. At finite temperature one generally calculates the heavy quark free energy [18] from correlation functions of Polyakov loops $L(\vec{n})$,

$$\mathrm{e}^{-V(r,T)/T} \equiv \langle \mathrm{Tr}L(\vec{0})\mathrm{Tr}L^\dagger(\vec{n})\rangle \quad , \quad rT = |\vec{n}|N_\tau \ , \tag{5}$$

where N_τ denotes the temporal extent of the lattice. At finite temperature the static $q\bar{q}$-pair can be in a singlet or octet state and the above correlation function thus only provides a thermal average over singlet and octet free energies,

$$\mathrm{e}^{-V(r,T)/T} \equiv \frac{1}{9}\mathrm{e}^{-V_1(r,T)/T} + \frac{8}{9}\mathrm{e}^{-V_8(r,T)/T} \quad . \tag{6}$$

Although $V_1 \equiv -8\,V_8$ in leading order perturbation theory, we do in general have to deal with both contributions to $V(r,T)$ and cannot directly extract the singlet component. Nonetheless the latter will dominate at short distances as well as at low temperature.

The colour averaged heavy quark free energy defined by Eq. 5 thus yields only indirect information for the discussion of thermal effects on heavy quark bound states. Nonetheless it reflects basic properties like the strong Debye screening of the $q\bar{q}$-pair above T_c. This has been analyzed in detail in the pure SU(3) gauge theory [19]. Additional screening effects do arise in QCD from the presence of light quarks. In addition to quantitative changes in the values of screening lengths the most significant changes occur in the long distance behaviour of $V(r,T)$. While in the pure gauge sector screening of the heavy quark free energy sets in only above T_c, i.e. $\lim_{r\to\infty} V(r,T)$ remains finite only for $T \geq T_c$, this is the case at all temperatures as soon as $m_q < \infty$. The temperature dependence of this screening effect, which arises from the spontaneous creation of $q\bar{q}$-pairs in the heat bath, is shown in Figure 6.

As can bee seen the free energy seems to reach a limiting form for $T \lesssim 0.6\ T_c$. For these temperatures it agrees with the confining Cornell type potential up to distances $r\sqrt{\sigma} \simeq 1.5$, i.e. $r \simeq 0.8$ fm. With increasing temperature this point is shifted to smaller distances. For $T \simeq 0.95\ T_c$ screening sets in already for $r\sqrt{\sigma} \simeq 0.8$ or $r \simeq 0.4$ fm. This clearly will also have an impact on heavy quark bound states. However, to quantify this we need further information on the short distance properties of the heavy quark free energy which should allow to disentangle contributions from the singlet and octet components.

5. Thermal Masses

The analysis of the temperature dependence of hadron properties, e.g. their masses and widths, is of central importance for our understanding of deconfinement and chiral symmetry restoration at T_c. Thermal modifications of the heavy quark potential which have been discussed above influence the spectrum of heavy quark bound states. Their experimentally observed suppression [20] thus is expected to be closely linked to the deconfining properties of QCD above T_c [21]. Changes in the chiral condensate, on the
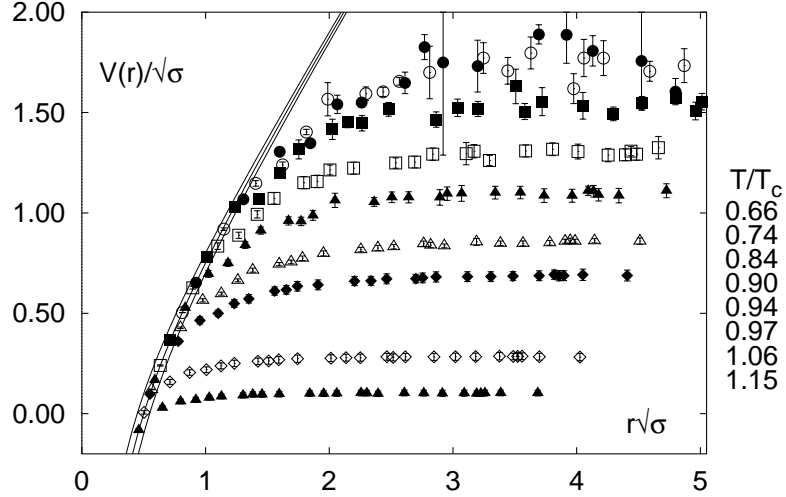
Figure 6. Temperature dependence of the heavy quark free energy in 3-flavour QCD [11]. The band of solid curves shows the Cornell potential $V(r) = -\alpha/r + \sigma r$ with $\alpha = 0.25 \pm 0.05$. The finite temperature free energies have been normalized to this potential at the shortest distance available, *i.e.* at $rT = 0.25$.

other hand, influence the light hadron spectrum and may result in experimental signatures, for instance in the enhanced dilepton production observed in heavy ion experiments [22].

In numerical calculations on Euclidean lattices one has access to thermal Green's functions $\bar{G}_H(\tau, \vec{r})$ in fixed quantum number channels H, to which in particular at high temperature many excited states contribute. As the temporal direction of the Euclidean lattice is rather short at finite temperature one usually has restricted numerical investigations to the analysis of the long distance behaviour of spatial correlations functions, $\bar{G}_H(\tau, \vec{r}) \sim \exp(-\bar{m}_H |\vec{r}|)$, which defines hadronic screening masses $\bar{m}_H$. This indeed gives evidence for the restoration of chiral symmetry above T_c, e.g. one finds that scalar and pseudo-vector screening lengths become degenerate and also the difference between screening lengths in scalar and pseudo-scalar channels strongly diminishes, which gives indications for a partial restoration of the $U_A(1)$ symmetry [1].

In order to get information on the T-dependence of pole masses and their widths one has to analyze the structure of temporal correlation functions. The information on hadron masses and quasi-particle excitations is then encoded in the spectral function $\sigma_H(\omega, \vec{p})$,

$$G_H(\tau, \vec{p}) = \int d^3r \, \exp\left(i \, \vec{p} \, \vec{r}\right) \bar{G}_H(\tau, \vec{r}) = \int_0^\infty d\omega \, \sigma_H(\omega, \vec{p}) \, \frac{\cosh(\omega(\tau - \beta/2))}{\sinh(\omega\beta/2)} \quad . \qquad (7)$$

At finite temperature the temporal correlation function usually is determined only at a small number of lattice grid points as the temperature is related to the finite extent of the lattice in this direction, $N_\tau = 1/(aT)$. A way out may be the use of anisotropic lattices [23]. These calculations indeed show large changes in meson correlators in the vicinity of T_c. To what extent the results suggest that pole masses in light meson channels exist as well defined states even above T_c, however, is difficult to judge solely on the basis of standard analysis techniques also used for correlation functions at zero temperature. At
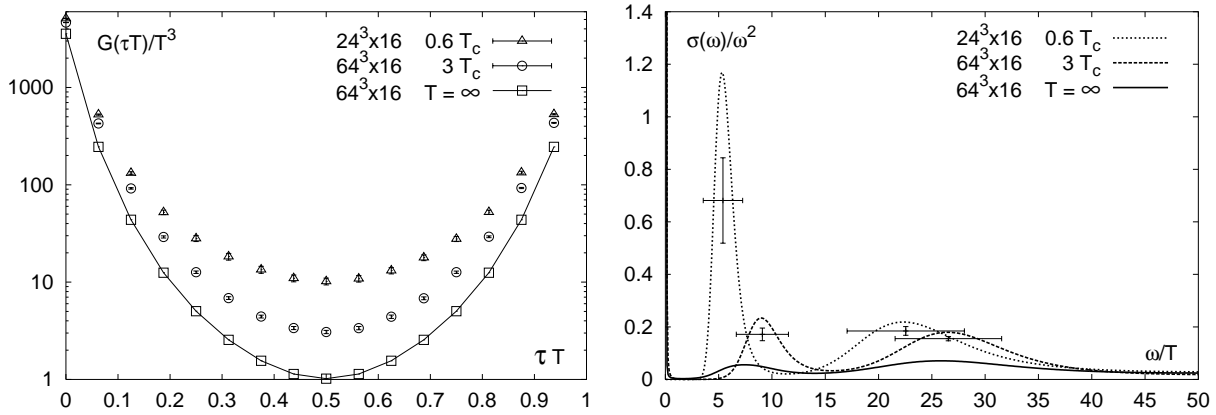
Figure 7. A first attempt to reconstruct the thermal pseudo-scalar spectral function (right) from the temporal correlation function (left) calculated within the static approximation of QCD at $T = 0.6T_c$ and $3T_c$ on lattices of size $24^3 \times 16$ and $64^3 \times 16$, respectively [28].

high temperature refined statistical techniques like the maximum entropy method [24] may be of help. It has recently been shown that this does allow to extract directly the spectral functions of hadron correlators [25,26] at $T = 0$ as well as high temperature [27]. A first attempt to use this approach for the determination of the pseudo-scalar spectral function below and above T_c is shown in Figure 7. This clearly reflects the drastic, qualitative change which occurs in the pseudo-scalar channel when one crosses T_c. The Goldstone pole which is present in the spectral function below T_c disappears in the plasma phase. Of course, this has to be analyzed more quantitatively in the future.

6. Conclusions

We have focused in this review on the calculation of basic thermodynamic quantities which are of immediate interest to experimental searches for the Quark Gluon Plasma.

Calculations of the QCD transition temperature which are based on different discretization schemes do provide a rather consistent picture. Extrapolations to the chiral limit are in good agreement and suggest a transition temperature of about 175 MeV in 2-flavour QCD. The numerical results obtained so far suggest a rather weak quark mass and flavour dependence of T_c. This also holds true for the critical energy density, which for 2-flavour QCD is estimated to be $\epsilon_c \simeq 700$ MeV and thus is of similar magnitude as that found already in the pure gauge sector. However, the error on ϵ_c still is about 50% and mainly is due to the current uncertainty on T_c which is estimated to be about 10%.

An analysis of the heavy quark free energy below T_c shows that screening effects increase significantly already below T_c. While the spontaneous creation of $q\bar{q}$-pairs leads to screening of the heavy quark potential at $r \simeq 0.8$ fm at low temperature this starts already at $r \simeq 0.4$ fm for $T \simeq 0.95T_c$.

We do have reached some understanding of thermal effects on hadron properties. In particular, modifications of the light meson spectrum due to flavour and approximate $U_A(1)$ symmetry restoration have been established. Indications for medium effects on pole masses have been found in an analysis of spectral functions. However, at present

these calculations are not detailed enough to be confronted with experimental data.

Of course, there are many other important issues which have to be addressed in the future. Even at vanishing baryon number density we do not yet have a satisfactory understanding of the critical behaviour of 2-flavour QCD in the chiral limit and the physically realized situation of QCD with two light, nearly massless quarks and a heavier strange quark has barely been analyzed. Moreover, the entire phase diagram at non-zero baryon number density is largely unexplored. An interesting phase structure is predicted in this case which currently is not accessible to lattice calculations.

REFERENCES

1. F. Karsch, Nucl. Phys B (Proc. Suppl.) 83-84 (2000) 14.
2. S. Ejiri, Nucl. Phys B (Proc. Suppl.) 94 (2001) 19.
3. C. Bernard et al., Phys. Rev. D60 (2000) 054503 and references therein.
4. A. Ali Khan et al. (CP-PACS), Phys. Rev. D63 (2001) 034502.
5. K.M. Bitar et al., Phys. Rev. D43 (1991) 2396.
6. C. Bernard et al., Phys. Rev. D56 (1997) 5584 and references therein.
7. R.G. Edwards and U.M. Heller, Phys. Lett. B462 (1999) 132.
8. N. Christ, private communication.
9. F. Karsch, A. Peikert and E. Laermann, hep-lat/0012023.
10. H. Meyer-Ortmanns and B.-J. Schaefer, Phys. Rev. D53 (1996) 6586;
    J. Berges, D.U. Jungnickel and C. Wetterich, Phys. Rev. D59 (1999) 034010.
11. F. Karsch, A. Peikert and E. Laermann, Phys. Lett. B478 (2000) 447.
12. H. Wittig, Int. J. Mod. Phys. A12 (1997) 4477.
13. B. Kastening and C. Zhai, Phys. Rev. D52 (1995) 7232.
14. A. Peshier, B. Kämpfer, O.P. Pavlenko, and G. Soff, Phys. Rev. D54 (1996) 2399;
    P. Lévai and U. Heinz, Phys. Rev. C57 (1998) 1879;
15. for a review see J.-P. Blaizot and E. Iancu, hep-ph/0101103.
16. A. Ali Khan et al. (CP-PACS), hep-lat/0103028.
17. C. Bernard et al., Phys. Rev. D55 (1997) 6861.
18. L. McLerran and B. Svetitsky, Phys. Rev. D24 (1981) 450.
19. O. Kaczmarek et al., Phys. Rev. D62 (2000) 034021.
20. M.C. Abreu et al. (NA50), Phys. Lett. B477 (2000) 28.
21. H. Satz, Rept. Prog. Phys. 63 (2000) 1511.
22. G. Agakishiev et al. (CERES), Phys. Rev. Lett. 75 (1995) 1272 and Phys. Lett. B422 (1998) 405.
23. Ph. de Forcrand et al. (QCDTARO), Phys. Rev. D63 (2001) 054501.
24. M. Jarell and J.E. Gubernatis, Phys. Rep. 269 (1996) 133.
25. Y. Nakaharai, M. Asakawa and T. Hatsuda, Phys. Rev. D60 (1999) 091503 and hep-lat/0011040.
26. see also contribution by T. Hatsuda to this conference.
27. I. Wetzorke and F. Karsch, hep-lat/0008008.
28. F. Karsch, E. Laermann, P. Petreczky, S. Stickan and I. Wetzorke, work in progress.